

## Visual focusing and levelling towards optical inspection of Mini/MicroLED panels

Hui Tang<sup>1</sup>, Yuzhang Wei<sup>2</sup>, Xiaoxian Ou<sup>2</sup>, Yingjie Jia<sup>2</sup>, Yanling Tian<sup>1</sup>

<sup>1</sup>School of Engineering, The University of Warwick; Coventry, UK

<sup>2</sup>Electromechanical engineering, Guangdong University of Technology, Guangzhou, China

Hui.Tang.4@warwick.ac.uk; yzwei@gdut.edu.cn; 2112201468@mail2.gdut.edu.cn; yingjiejia1996@163.com; Y.Tian.1@warwick.ac.uk

### Abstract

In order to improve the focus quality and efficiency of Mini/MicroLED chip panel defect detection, we focus our research on visual focusing and levelling techniques. This paper reports on the construction of Image focus evaluation method based on Gaussian fuzzy difference (F-GFD), and the method of focus adjustment and leveling based on ZTT $\theta$  leveling and correcting motion stage is also proposed. By optimising and adjusting the parameters, the image focus evaluation method (F-GFD) has a high focus resolution and high sensitivity effect, which has an axial resolution better than 1.25  $\mu\text{m}$  axial resolution. Experiments show that the image focus evaluation method (F-GFD) combined with ZTT $\theta$  stage can realize multi-points focus of Mini/MicroLED panel and the leveling process of panel and image plane, which further provides a basis for solving the defocus problem caused by panel warping in the defect detection of Mini/MicroLED chips.

Focusing and leveling; Image focus evaluation; Gaussian fuzzy difference; Mini/MicroLED panels.

### 1. Introduction

Focusing and leveling is one of the important processes in display semiconductor manufacturing, which can compensate the errors caused by defocusing to ensure the quality of imaging, processing and improve the production yield of the circuit<sup>[1]</sup>.

In the traditional optical system, CCD and laser generator are usually used to measure the height according to the triangle method to determine the defocus amount<sup>[2]</sup>. In recent years, Jian Wang et al. proposed grating shear interferometry to determine the out-of-focus amount and tangent slope of wafer by measuring the phase difference<sup>[3]</sup>. Canon and ASML companies used photoelectric detection array, CCD array and other detectors to achieve focusing and leveling measurement in the way of grating array and spot array. Nikon proposed to reduce the ASD error by placing polarizer between the lens and the silicon wafer to improve the process adaptability of the focusing and leveling system, which detects the light intensity of each polarization<sup>[4]</sup>. The gain coefficient of the focusing and leveling sensor is simulated and tested by the Institute of Microelectronics of the Chinese Academy of Sciences<sup>[5]</sup>. The results showed that the calibration sensor system can effectively reduce the variation of thickness of different materials of semiconductor panels. Yonghong Wang proposed a new focusing algorithm to complete the focusing process of TFT-LCD panels and improved efficiency<sup>[6]</sup>.

In general, there were two dominant approaches to solving the focus levelling problem, one is the principle based on measuring surface height by optical triangulation and the other is to ensure defocus amount by adding sensors. For the display panels, active focusing or passive focusing is basically adopted for single position focusing, but there are few studies on multi-point focusing or focusing and leveling of the display panel. Therefore, in order to solve the problem of defocusing due to panel warping in Mini/MicroLED chip defect detection, the image focus evaluation method based on Gaussian fuzzy

difference is proposed, and the feasibility of focusing and leveling technology is verified by combining with ZTT $\theta$  leveling and correcting stage.

### 2. Image focus evaluation method based on Gaussian fuzzy difference (F-GFD)

#### 2.1 Fuzzy formation and mechanism of defocusing imaging

In the optical imaging model, the object to be measured will present different clarity basing on its own location in the visual system. With the movement along the direction of the optical axis, there will be sharp to blur with out-of-focus amount changes. The optical imaging simplified model shown in Fig. 1.

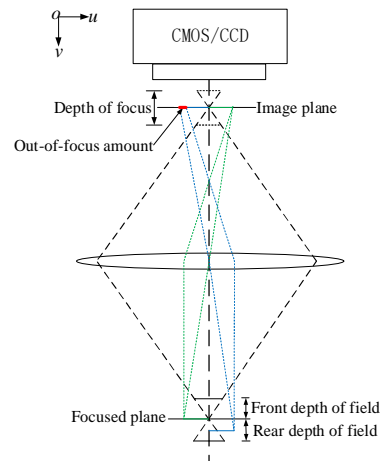


Figure 1. Simplified model of optical imaging

At the same time, the process of focusing to defocusing can be regarded as the process of transforming the focused image through a certain degenerate model. Thus, without considering linear space, the defocused imaging model can be expressed simplistically as:

$$F_i(x, y) = F(x, y) \times h_t(x, y) \quad (1)$$

From(1), the subscript  $i$  is the sequence number corresponding to the position moved along the optical axis direction;  $F(x, y)$  is the focused image;  $F_i(x, y)$  is the image acquired at the position corresponding to sequence number  $i$ ;  $h_i(x, y)$  is the degenerated model corresponding to  $F(x, y)$ .

In practice, due to the existence of a certain symmetry between the foreground depth and the background depth, the degenerate model is fitted by a Gaussian function. The degree of degradation is determined by the size of the standard deviation  $\sigma_i$ , so that the larger the standard deviation will have higher degree of fuzzy and degradation. The representation of image is usually a two-dimensional discrete signal, so  $h_i(x, y)$  can be represented by a two-dimensional Gaussian function:

$$h_i(x, y) = \frac{1}{\sqrt{2\pi}\sigma_i} \exp\left[-\frac{x^2 + y^2}{2\sigma_i^2}\right] \quad (2)$$

## 2.2. Addition of Gaussian fuzzy difference

From 2.1, it can be understood that the key of visual focusing technique makes the object under test in the focusing plane so that it can be clearly imaged. Among them, the sharpness evaluation value obtained by the image focus evaluation method will be an important basis for judging whether it is located in the focus plane.

A Gaussian kernel convolution operation with a determined standard deviation is performed on the images acquired by the vision system, in other words, Gaussian blur is added to the original imaging model. Therefore, the image obtained from the out-of-focus imaging model in Section 2.1 by blurring the Gaussian again is  $f_i(x, y)$ , which can be expressed as<sup>[7]</sup>:

$$f_i(x, y) = F_i(x, y) \times h(x, y) = F(x, y) \times h_i(x, y) \times h(x, y) \quad (3)$$

From (3):  $h(x, y)$  is the Gaussian kernel convolution whose standard deviation has been determined.

Eq.  $h_i(x, y) * h(x, y)$  can be written as an expression in accordance with the principle of multiplication of Gaussian convolution kernel:

$$h_i(x, y) \times h(x, y) = \frac{1}{\sqrt{2\pi} \cdot \sqrt{\sigma_i^2 + \sigma^2}} \exp\left[-\frac{x^2 + y^2}{2(\sigma_i^2 + \sigma^2)}\right] \quad (4)$$

From (4), the standard deviation of the new Gaussian convolution kernel is  $\sqrt{\sigma_i^2 + \sigma^2}$ , which can be compared with the standard deviation of the out-of-focus imaging model in (2) and the standard deviation of completely fuzzy imaging model to obtain the magnitude relation, denoted as:

$$\sigma_i \leq \sqrt{\sigma_i^2 + \sigma^2} \leq \sigma_{\text{dim}} \quad (5)$$

From (5),  $\sigma_{\text{dim}}$  is the standard deviation of the Gaussian convolution kernel used to make the focused image  $F(x, y)$  completely fuzzy. According to the way of adding the standard deviation of the Gaussian kernel convolution operation, it had already determined the standard deviation of the new Gaussian convolution kernel is  $\sqrt{\sigma_i^2 + \sigma^2}$  can only be constantly converged to  $\sigma_{\text{dim}}$ .

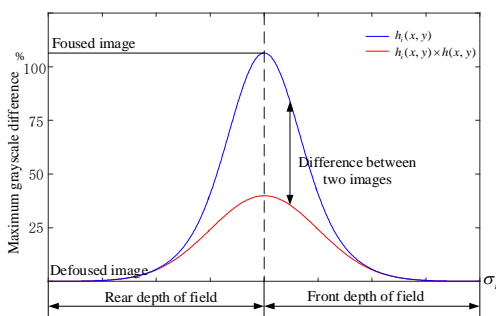


Figure 2. Comparison of grey scale difference between images before and after processing

According to Section 2.1, the larger the standard deviation of the Gaussian convolution kernel is, the more significant the blurring effect on the image. Therefore, for the image joining the Gaussian kernel convolution operation whose standard deviation has been determined, the comparison of grey scale difference values before and after processing will be shown in Fig. 2.

The blue curve in Figure 2 is the expression of the original out-of-focus imaging fuzzy model in the form of grey scale difference, because the change of  $\sigma_i$  makes a series of images in the focusing plane, in the two directions of front and rear depth of field to show a tendency to reduce the value of maximum grayscale difference respectively (have a gradually blurring tendency). The red curve represents the original out-of-focus imaging fuzzy model added to the Gaussian kernel convolution of standard deviation has been determined after the formation of the model, the standard deviation of the standard deviation  $\sqrt{\sigma_i^2 + \sigma^2}$  will decide to images in the focusing plane, respectively, the grey scale difference show a similar tendency as blue curve in the two directions of front and rear depth of field.

Combining the equation (5) with the comparison of the red and blue curves, it can be clearly seen that if the acquired image is in-focus, the image after the second Gaussian convolution will have obvious grey value differences (obvious blurring). If the acquired image is out-of-focus, the grey value difference (blurring) of the image after the second Gaussian convolution change less. Therefore, the grey value differences (blurring) decrease with the increase of out-of-focus amount. The difference between the blurred image and the original image can be used as a criterion for sharpness evaluation and as a basis for defining the focus position.

The difference between  $F_i(x, y)$  and  $f_i(x, y)$  is caused by processing after quadratic Gaussian convolution, so the value of the standard deviation of the Gaussian convolution sum has a close relationship with the sensitivity of the algorithm, and at the same time, in order to satisfy the stability of the Gaussian kernel matrix operation, there is the following relationship between the Gaussian convolution kernel and the mask size<sup>[8]</sup>:

$$\sigma = 0.3 \left[ \left( \frac{k_{\text{size}} - 1}{2} \right) - 1 \right] + 0.8 \quad (6)$$

From (6),  $k_{\text{size}}$  is the mask size size, so the value needs to be taken to satisfy that the equation holds.

The difference between  $F_i(x, y)$  and  $f_i(x, y)$  can be expressed by the difference between the global variance values of the two images, then the clarity evaluation result of a single image can be expressed as:

$$\text{Diff} = \text{abs}\{\text{cov}[F_i(x, y)] - \text{cov}[f_i(x, y)]\} \quad (7)$$

From (7),  $\text{Diff}$  is the difference of the variance value, and also represents the clarity evaluation result of the image;  $\text{cov}(\ast)$  means calculating the global variance of the image;  $\text{abs}(\ast)$  means taking the absolute value.

According to the relationship between the values of equation (6), if the Gaussian standard deviation is taken as 0.8, 1.1, 1.4, 1.7, the mask size of the Gaussian convolution kernel should be 3\*3, 5\*5, 7\*7, 9\*9 respectively. So the completeness of the convolution operation can be guaranteed according to this principle. The difference between the images before and after processing is calculated through the arithmetic relationship of the equation (7) to obtain the clarity evaluation value, and the results for the same set of images processing are shown in Fig. 3.

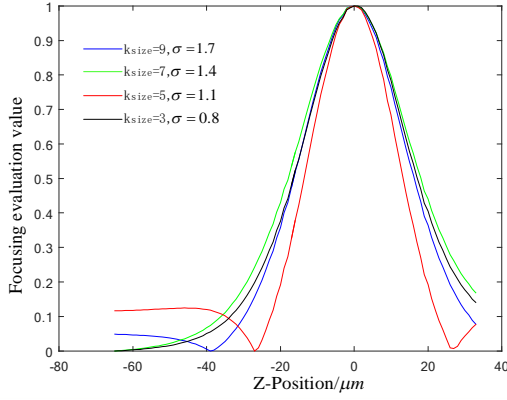


Figure 3. Clarity evaluation results after different Gaussian standard deviation treatments

### 2.3. Algorithm Effectiveness Validation and Focused Evaluation Metrics

Prior to this, many researchers have proposed spatial domain-based focus evaluation algorithms, including the most common gradient sum-of-squares function (Sobel operator), gradient filtering function (Brenner operator), and Laplace function, and these traditional focus evaluation methods are also the most commonly used in the industry. Therefore, we propose an image focusing evaluation method based on Gaussian fuzzy difference to compare with traditional algorithms by means of quantitative evaluation, highlighting our advantages and indicators. Suppose the image size is  $m \times n$ :

- (1) Gradient filter function (Brenner operator)

$$F_{Brenner} = \sum_{i=1}^m \sum_{j=1}^n [p(i, j+2) - p(i, j)]^2 \quad (8)$$

- (2) Gradient sum-of-squares function (Sobel operator)

$$F_{Sobel} = \frac{1}{m \cdot n} \sum_{i=1}^m \sum_{j=1}^n \{ [p(i, j) \times G_x]^2 + [p(i, j) \times G_y]^2 \} \quad (9)$$

$$G_x = \begin{bmatrix} -1 & -2 & -1 \\ 0 & 0 & 0 \\ 1 & 2 & 1 \end{bmatrix} \quad G_y = \begin{bmatrix} -1 & 0 & 1 \\ -2 & 0 & 2 \\ -1 & 0 & 1 \end{bmatrix} \quad (10)$$

- (3) Laplace function (Laplacian operator)

$$F_{Laplace} = \frac{1}{m \cdot n} \sum_{i=1}^m \sum_{j=1}^n [p(i+1, j) + p(i-1, j) + p(i, j+1) + p(i, j-1) - 4 \cdot p(i, j)]^2 \quad (11)$$

In accordance with Figure 2 effect comparison, the image focus evaluation method based on Gaussian fuzzy difference selects the fuzzy form with a mask size of  $5 \times 5$  and a standard deviation of 1.1. The result obtained is plotted as a curve, which compared with the gradient sum-of-squares function, the gradient filter function, and the Laplacian function (as shown in Fig. 5).

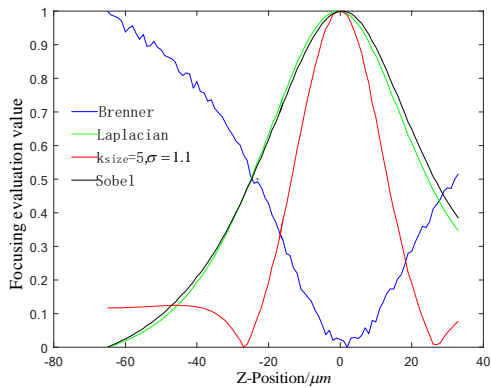


Figure 4. Comparison of the effect of different clarity functions

Based on the statement of the Heisenberg uncertain principle and emulation of the autofocusing uncertainty measure<sup>[9]</sup>, focus resolution can be defined by<sup>[10]</sup>:

$$\sigma^2 = \frac{1}{\|f\|^2} \int_{-\infty}^{+\infty} [(x - x_p) \cdot f(x)]^2 dx \quad (12)$$

Conversion of integral form to discrete point superposition form:

$$\sigma^2 = \frac{1}{\|f\|^2} \sum_{i=1}^n [(i - i_p) \cdot f(i)]^2 \quad (13)$$

The computed  $\sigma^2$  for different clarity functions shown in Figure 4 are listed in Table 1. From Table 1, we can clearly see that the  $\sigma^2$  of Image focus evaluation method based on Gaussian fuzzy difference is significantly lower than other focus functions. This means that Image focus evaluation method based on Gaussian fuzzy difference has higher focus resolutions.

Table 1 Computed focus resolutions for Fig.4

Focus Measure	Sobel	Lapacain	F-GFD
$\sigma^2$	425.965	447.542	150.008

### 3. Mini/MicroLED panels focusing and levelling process implementation

In Mini/MicroLED AOI chip defect inspection and other pan-semiconductor equipment, Mini/MicroLED panels are placed on the fixture and then transported to the workstation. Due to assembly problems and the panel warping phenomenon, Mini/MicroLED panels are not completely in the depth of field range and parallel to the camera's datum surface, which affects the inspection accuracy and efficiency. So it is necessary to adjust so that the panel is parallel to the focal plane.

#### 3.1 Focusing plane positioning accuracy experiment

In order to verify the ability of the image focus evaluation method based on Gaussian fuzzy differences to layer along the optical axis direction (resolution of slice images).

The experimental (Fig. 5) system consists of a vision system with a Z-direction objective displacement stage. The objective lens in the vision system is CCW-10x, which has a magnification of 10, a numerical aperture of 0.28, and a depth of field of 3.5  $\mu\text{m}$ . Z-axis repeatability is less than  $\pm 500\text{nm}$ .

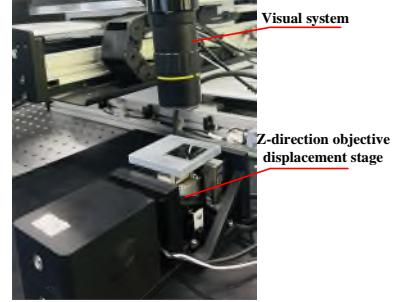


Figure 5. Positioning accuracy experiment

The system performs axial traversal scans and acquires images in 1.25  $\mu\text{m}$  steps over a range of  $\pm 20 \mu\text{m}$  near the plane of focus, followed by resolution performance metrics analysis (Fig. 6).

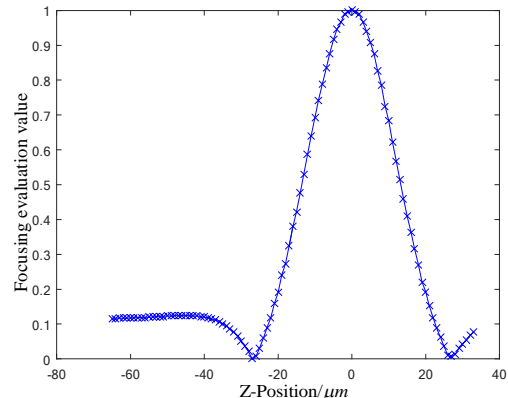


Figure 6. Z-axis resolution performance specification

The results are shown in Fig.6, it can indicate that when axial traversal scanning in the situation of  $1.25\mu\text{m}$  step, the image focus evaluation method ( F-GFD ) achieves axial position resolution within  $20\ \mu\text{m}$  before and after the focusing position. Therefore the axial resolution is considered to be better than  $1.25\ \mu\text{m}$ .

### 3.2 Focusing and levelling process

According to the motion characteristics of ZTT $\theta$  levelling and deskewing stage (Fig. 7) and the characteristics of focus levelling, the image focus evaluation method based on Gaussian fuzzy difference proposed in Chapter 2 is combined with ZTT $\theta$  levelling and deskewing stage to realise the Mini/MicroLED panel focus leveling process.

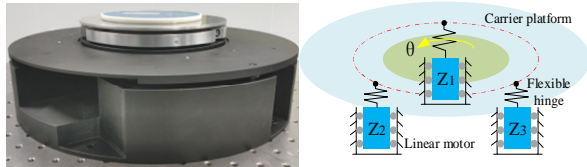


Figure 7. ZTT $\theta$  levelling and guiding stage and simple model

As shown in Figure 7, the ZTT $\theta$  levelling stage can achieve high-precision pitch and yaw, but it needs to implement the motion strategy in conjunction with vision algorithms ( F-GFD ) to reduce the influence of coupled and parasitic motions in the focusing and leveling process. This guarantees the completion of accurate focusing and leveling.

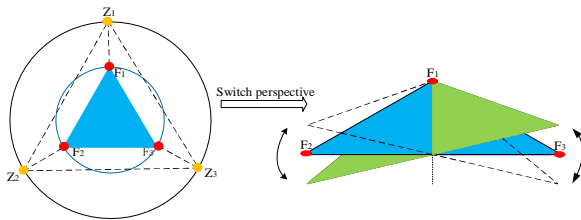


Figure 8. Schematic diagram of ZTT $\theta$  stage focusing and levelling movement

As shown in Figure 8,  $Z_1Z_2Z_3$  are the support points of the stage (drive point);  $F_1F_2F_3$  are the focus points, which located in the same arc and located in the radius of  $Z_1Z_2Z_3$ . Based on the existing positional relationship, the position height change of  $F_1F_2F_3$  can be inverted to solve the pending motion of the support point  $Z_1Z_2Z_3$  based on the motion position mapping relation. If  $F_2$  and  $F_3$  do the movement in the opposite direction, the plane composed of  $F_1F_2F_3$  is swinging on the axis of the centre line where  $F_1$  is located, theoretically, the position of  $F_1$  can be kept highly unchanged to achieve decoupling. The following movement process and strategy are also developed around this. The specific process is as follows:

1. Firstly, the three-axis synchronised motion is adjusted to achieve the optimum image clarity within the vision system (image clarity evaluation function) to obtain the position  $F_1$ ;
2. Keeping the height of  $Z_1$  unchanged, the system focuses on the  $F_2$  position to achieve optimal clarity through  $Z_2$  and  $Z_3$  for the opposite way of movement (the plane movement state is shown in Fig. 8 on the right). The  $Z_2$  height position is recorded after the focus search was completed;
3. Continue to keep the height of  $Z_1$  unchanged, the system focuses on the  $F_3$  position to achieve optimal clarity through  $Z_2$  and  $Z_3$  for the opposite way of movement. The  $Z_3$  height position is also recorded after the focus search was completed;
4.  $Z_2Z_3$  were reached before the recorded position, focusing and levelling process is complete.

By reproducing the above focus levelling strategy in the host computer, the overall process of focus levelling is completed in the experimental system (Fig. 9).

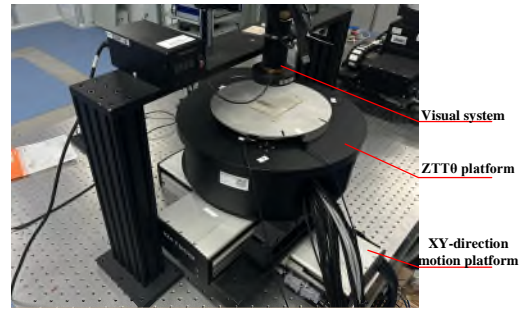


Figure 9. Integral focusing and levelling experiment system construction

From the results, the difference in the sharpness evaluation value of the focusing area  $F_1F_2F_3$  is very small and all of them can reach a clear state. Therefore, it is shown that the image focus evaluation method based on Gaussian fuzzy difference ( F-GFD ) in conjunction with the ZTT $\theta$  levelling and deviation correction stage can complete the overall process of focus levelling.

## 4. Summary

The image focus evaluation method based on Gaussian fuzzy difference ( F-GFD ) proposed in the paper can achieve axial resolution better than  $1.25\ \mu\text{m}$ , and the peak and focus resolution are improved compared with the traditional way. At the same time the focus evaluation method counts with the ZTT $\theta$  levelling and deskewing stage in conjunction with the focus leveling technology is able to complete the Mini/MicroLED panel focus leveling process, which provides a certain basis for solving the problem of Mini/MicroLED out of focus due to panel warping. Moreover, it has the advantage of lower cost and simpler operation process than the traditional optical triangulation principle or additional sensors.

## Acknowledgment

The authors are thankful to the funding of the European Union's Horizon 2020 research and innovation programme under the Marie Skłodowska-Curie Grant agreement no. 101026104.

## References

- [1] Boef, D. and J. Arie, Optical wafer metrology sensors for process-robust CD and overlay control in semiconductor device manufacturing. *Surface Topography Metrology & Properties*, 2016. 4(2): 023001.
- [2] Huang T , Liu S , Yi P , et al. Focusing and leveling system for optical lithography using linear CCD[J]. *Proceedings of SPIE - The International Society for Optical Engineering*, 2009, 7160(2):-.
- [3] Wang, J., S. Hu and X. Zhu, Measurement of Wafer Focus by Grating Shearing Interferometry. *Applied Sciences*, 2020. 10(21): p. 7467.
- [4] Hidaka, Y., K. Uchikawa and D.G. Smith, Error analysis and compensation method of focus detection in exposure apparatus. *Optical Society of America*, 2009(1).
- [5] Sun, Sangsang, Wang, Dan & Zong, Mingcheng, Process correlation study of gain coefficients of focus levelling sensors. *Journal of Optics*, 2022. 42(04): p. 109-116.
- [6] Wang, Y. H. et al, Research and comparison of auto-focusing algorithms for optical inspection of TFT-LCD panels. *Liquid Crystal and Display*, 2016. 31(4): p. 8.
- [7] David, et al., Blind image blur assessment by using valid reblur range and histogram shape difference. *Signal Processing Image Communication*, 2014.
- [8] Yuan T. et al, A double blur based focus evaluation method for microscopic images. *Journal of Optics*, 2023. 43(10): p. 63-72.
- [9] Yang, G. and B.J. Nelson. Wavelet-based autofocusing and unsupervised segmentation of microscopic images. in *IEEE/RSJ International Conference on Intelligent Robots & Systems*. 2003.
- [10] Zong, G.H., et al., Research on Wavelet Based Autofocus Evaluation in Micro-vision. *Chinese Journal of Aeronautics*, 2006. 19(3): p. 239-246.